Amplitude wave in one-dimensional complex Ginzburg–Landau equation

Xie Ling-Ling (谢玲玲), Gao Jia-Zhen (高加振),
Xie Wei-Miao (谢伟苗), and Gao Ji-Hua (高继华)†

Shenzhen Key Laboratory of Special Functional Materials, College of Materials, Shenzhen University, Shenzhen 518060, *China*

(Received 11 April 2011; revised manuscript received 24 June 2011)

The wave propagation in the one-dimensional complex Ginzburg–Landau equation (CGLE) is studied by considering a wave source at the system boundary. A special propagation region, which is an island-shaped zone surrounded by the defect turbulence in the system parameter space, is observed in our numerical experiment. The wave signal spreads in the whole space with a novel amplitude wave pattern in the area. The relevant factors of the pattern formation, such as the wave speed, the maximum propagating distance and the oscillatory frequency, are studied in detail. The stability and the generality of the region are testified by adopting various initial conditions. This finding of the amplitude pattern extends the wave propagation region in the parameter space and presents a new signal transmission mode, and is therefore expected to be of much importance.

Keywords: wave propagation, complex Ginzburg–Landau equation, amplitude wave

PACS: 05.45.–a, 82.40.Ck, 42.25.Bs **DOI:** 10.1088/1674-1056/20/11/110503

1. Introduction

Spatiotemporal systems are rich reservoirs of diverse pattern formations and complexities of natural phenomenology.[1,2] In this respect, the characteristic of a wave medium in an extended system is an important research topic and it has attracted much attention in the relevant scientific communities.[2−10] The study of signal propagation in different spatiotemporal systems is directly relevant to the information spreading and the applications in real systems and therefore is a research field of much importance.[11−16] In addition, the wave is one of the oldest research notions in the scientific development and it is a basic concept used to understand our universe. Recently, a class of coherent structures called modulated amplitude waves (MAWs) have been recognized by Brusch *et al.*[17−19] The MAWs are quasi-periodic solutions of the complex Ginzburg–Landau equation (CGLE), and their saddle-node bifurcations relate to the transition from the phase to the defect chaos. The existence and the stability of the MAW have been proved in many cases.[20,21] In the published research work, the signal propagation is studied in different media and many new features of the complex wave modes are revealed. From this viewpoint, the amplitude variation wave in the CGLE is one important coherent structure with many potential applications. In this work, we consider the one-dimensional CGLE, which is a spatiotemporal model studied extensively in the past several decades, and investigate the signal propagation to uncover a novel type of amplitude wave.

2. Model and numerical results

In the one-dimensional case, the CGLE is in the form of[1]

$$\partial_t A = A + (1 + \mathrm{i}c_1)\,\partial_x^2 A - (1 + \mathrm{i}c_2)\,|A|^2 A, \qquad (1)$$

where $A = A(x,t)$ is a complex variable, c_1 and c_2 are real system parameters. System (1) describes the onset of the supercritical Hopf bifurcations in a spatially extended system. It has been used to study pattern formations and the chaos control.[10,22−29] System (1) admits the following plane-wave solutions:

$$A(x,t) = \sqrt{1-k^2}\,\mathrm{e}^{\mathrm{i}(kx-\omega t)},$$
$$\omega = c_2 + (c_1 - c_2)\,k^2, \qquad (2)$$

where k is the wave number, and ω is the oscillatory frequency. The stability of the plane-wave solutions

†Corresponding author. E-mail: jhgao@szu.edu.cn

© 2011 Chinese Physical Society and IOP Publishing Ltd

has been confirmed by using a linear stability analysis. When

$$k^2 \leq k_{\max}^2 = \frac{1 + c_1 c_2}{2(1 + c_2^2) + 1 + c_1 c_2}, \tag{3}$$

the plane-wave solutions are stable. In addition, if $1 + c_1 c_2 < 0$ ($1 + c_1 c_2 = 0$ is called the Benjamin–Feir–Newell line, or the BFN line), all plane-wave solutions are unstable, and the system exhibits various spatiotemporal behaviours, including the defect turbulence, the phase turbulence, the spatiotemporal intermittency, and the bichaos, in a wide parameter region.[2−4,30]

Now we consider system (1) under the no flux boundary condition, and it is in a disordered state, which is plotted in Fig. 1(a). The spatial distribution of the variable is not periodic. A wave source is provided at boundary position $x = 0$, which is used to produce a periodic signal in the system. The orderly emitted wave is released from the source and propagates to occupy the whole system space (Figs. 1(b)–1(d)). This method has been used to suppress the spatiotemporal chaos and drive a system into the stationary state.[31] In Fig. 1, the stable signal spread is observed when system parameters $c_1 = 0.6$ and $c_2 = -0.6$ are adopted. The simulations are performed by using the explicit Euler method. The time iteration and the space step for the numerical simulations are $\Delta t = 0.005$ and $\Delta x = 0.5$, respectively. And the system size is $L = 1000$.

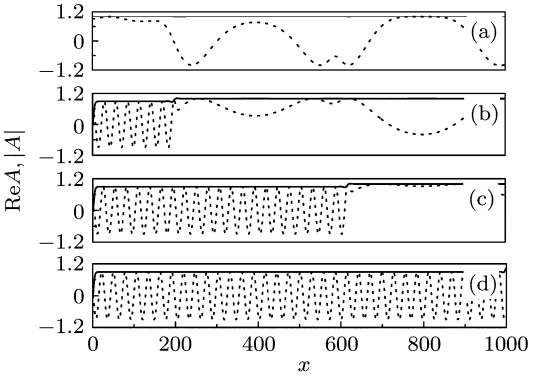


Fig. 1. Spatial distributions of Re$A(x,t)$ (dot line) and $|A|$ (solid line) with $c_1 = 0.6$, $c_2 = -0.6$, $L = 1000$, at (a) $t = 0$ (without control), (b) $t = 400$ (Re$A(x,t)$ presents periodic oscillation after setting a wave source $|A| = 0$ at boundary position $x = 0$), (c) $t = 800$, and (d) $t = 1200$ (the wave signal spreads and occupies the whole space).

3. Amplitude wave

It is an interesting question whether the stable signal propagation can be found when the system parameters are changed. In Fig. 2, the space–time evolutions of the magnitude of the system variable for different system parameters are plotted. For specificity and simplicity, we fix $c_1 = 0.6$ and inspect the different simulation results obtained with different system parameter c_2. In Fig. 2(a), $c_2 = -0.6$ is chosen, the amplitude of system variable $|A|$ is almost constant, only a slight variation from 0.9 to 1 is observed. The signal propagates from $x = 0$ to $x = L$ with a stable speed and finally spreads over the whole space. In Fig. 2(b), $c_2 = -1.24$, variable modulus $|A|$ can drop to near zero occasionally. Such a point is called a topological defect, which normally forms a zigzag structure in the spatially extended system.[32] In this case, the signal propagation is blocked by the defect points, and the mechanism of the good wave signal transmission is destroyed. In Fig. 2(c), $c_2 = -1.3$, an interesting phenomenon, i.e., a special mode of wave propagation, is revealed. In this case, although the defect points influence the stability of the signal, the wave can reach the whole space with an amplitude wave mode, which is different from the case shown in Fig. 2(a). When system parameter c_2 is -1.5, the result is illustrated in Fig. 2(d), more defect points can be observed, the state is essentially the same as that shown in Fig. 2(b), and we cannot find the signal propagation due to the existence of the defect points. The amplitude wave propagation shown in Fig. 2(c) is found to be different from the ordinary stable signal propagation shown in Fig. 2(a) and has more interesting features. To our best knowledge, it is a novel phenomenon and has not been reported in the published papers yet.

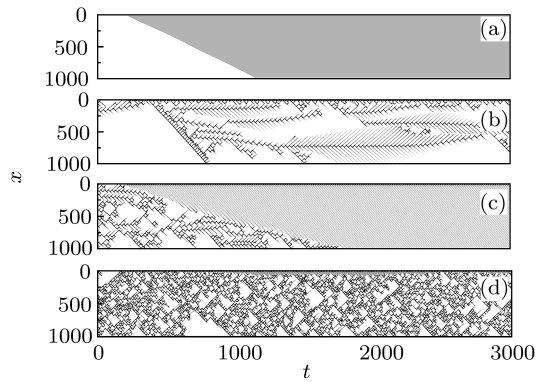


Fig. 2. Stable signal spreading with time shown by grey scale of $|A|$ (black corresponding to $|A| = 0$) for $c_1 = 0.6$, and $c_2 = -0.6$ (a), -1.24 (b), -1.3 (c), and -1.5 (d). The wave source is set at $t = 200$.

To confirm the existence of the special signal in Fig. 2(c), we compute the evolution of the variable with $c_1 = 0.6$ and $c_2 = -1.34$. The space distributions

of the system variable are depicted in Fig. 3. The initial real part Re$A(x,t)$ (dot line) and amplitude $|A|$ (solid line) are shown in Fig. 3(a), which clearly shows the chaotic motion. The wave source is set at $t = 200$. The approximately regular oscillation appears under the driving of the boundary wave source (Fig. 3(b)), and it spreads more widely in the system as the time goes by (Fig. 3(c)). Finally the signal spreads over the whole system space, which is illustrated in Fig. 3(d). The transmitted signals in Fig. 3 have different features from those displayed in Fig. 1. Firstly, the approximately periodic spatial distribution is obvious, which is far from that of the defect-mediated turbulent state shown in Fig. 2(b). Secondly, it is interesting that the periodic variation of the variable is similar to that of the MAWs. In this respect, the novelty of the wave propagation is confirmed.

Now we turn to the evolutions of the variable amplitudes for different system parameters. For a clearer comparison, we choose the same system parameter settings as those in Fig. 2. Amplitude $|A|$ and the phase space orbitals in the ReA–ImA plane of midpoint $x = L/2$ are shown in the left and the right columns of Fig. 4, respectively. In Figs. 4(a) and 4(b), the constant amplitude is observed with $c_2 = -0.6$, and the phase space orbital presents a simple cycle indicating the periodic trajectory. In Figs. 4(c) and 4(d), $c_2 = -1.24$, the amplitude is unstable, and the variable loses its periodicity. Correspondingly, the phase space behaviour is no longer of a simple cycle, and the chaotic trajectory is observed. In Figs. 4(e) and 4(f), $c_2 = -1.3$, $|A|$ presents the periodicity with a slight magnitude oscillation. A quasi-periodic torus is observed in the phase space, which is corresponding to the signal propagation found in Figs. 2(c) and 3. In Figs. 4(g) and 4(h), $c_2 = -1.5$, the whole system is covered by the spatiotemporal chaos.

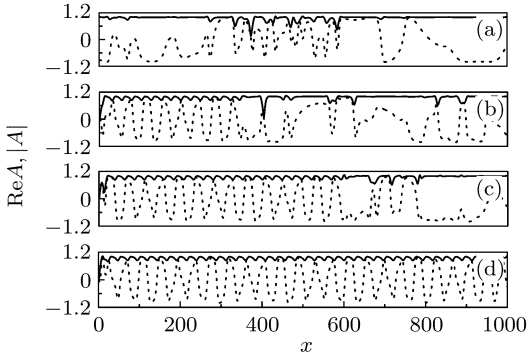


Fig. 3. Spatial distributions of Re$A(x,t)$ (dot line) and $|A|$ (solid line), with $c_1 = 0.6$, $c_2 = -1.34$, $L = 1000$, and $t = 0$ (without control) (a), 600 (b), 1200 (c), and 2000 (d). A novel amplitude wave occupies the whole system space.

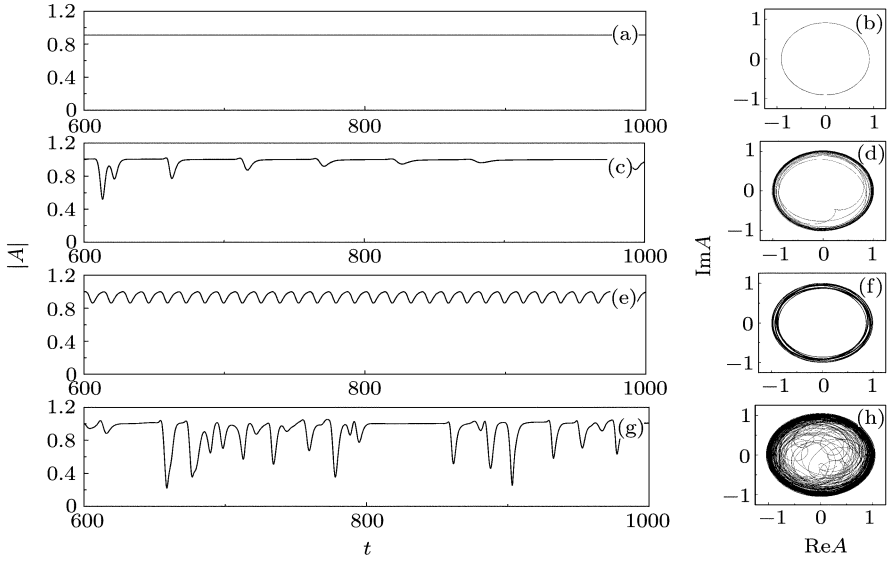


Fig. 4. Amplitude and phase space orbitals of the amplitude waves. Left column shows the amplitude versus time. Right column indicates the phase space orbitals in the ReA–ImA plane. Here we consider space position $x = L/2$, $c_1 = 0.6$, and $c_2 = -0.6$ ((a) and (b)), -1.24 ((c) and (d)), -1.3 ((e) and (f)), and -1.5 ((g) and (h)).

To gain an insight into the behaviour of the amplitude wave, we study the time series of ReA and $|A|$ and their corresponding intensities of the fast Fourier transform (FFT), which are shown in Fig. 5. The frequency characteristic is an important factor in the investigation of the signal propagation. There exists a basic frequency ω_0 (for example, $\omega_0 \approx 0.157$ for the parameter setting in Fig. 5). Several isolated frequency peaks are observed, which correspond to the integer multiples of the basic frequency. The highest

frequency peak is $\Omega_1 = 7\omega_0$ for ReA, and two lower peaks $\Omega_2 = \Omega_1 \pm 3\omega_0$ are found in the neighbourhood of Ω_1. The occurrence of Ω_2 with a small intensity is crucial for the stability of the special amplitude wave propagation. In this case, the system variable has the form

$$A = a\,\mathrm{e}^{\mathrm{i}\Omega_1 t} + b\,\mathrm{e}^{\mathrm{i}\Omega_2 t}, \tag{4}$$

where a and b are the frequency intensities contributed by Ω_1 and Ω_2, respectively. According to the simulation results shown in Fig. 5(b), $a >> b$, we have

$$|A| \approx a + b\cos(\Omega_1 - \Omega_2)\,t, \tag{5}$$

which is exactly the amplitude behaviour shown in Figs. 5(c) and 5(d). An interesting question is how the smaller frequency peak of Ω_2 comes into being. Recently, a novel spiral wave in a two-layer system has been reported, a similar Ω_2 has been demonstrated to be dependent on the coupling interactions between the two-layer spiral patterns.[33] In our observations, the new frequency Ω_2 is intuitively believed to originate from the boundary wave source. The boundary control is a fixed value point and does not introduce any new periodic signal injection, therefore the newly born Ω_2 has the same basic frequency ω_0, which is also a constructive element of the free system frequency Ω_1. Although the wave source does not provide any new frequency for the system, it changes the intensities for the frequencies. In this respect, the wave source plays an important role for the occurrence of the novel signal propagation.

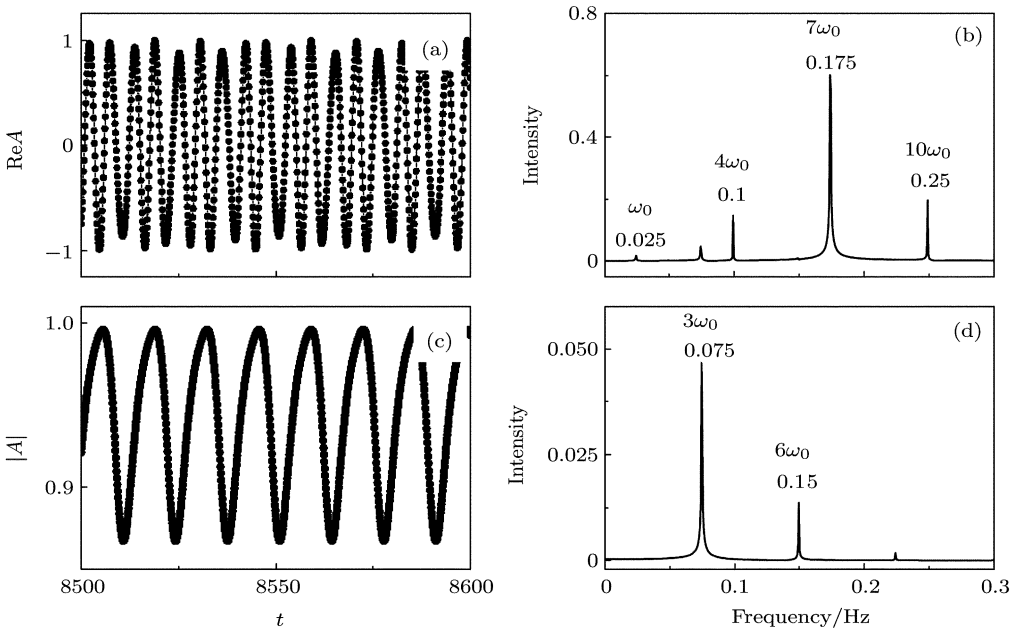


Fig. 5. Time series of variables and their corresponding FFTs with $c_1 = 0.6$ and $c_2 = -1.3$. Panels (a) and (b) show ReA versus time and the corresponding frequency spectrum respectively. Panels (c) and (d) show $|A|$ versus time and the corresponding frequency spectrum respectively.

We show the category of the signal propagation in the c_1–c_2 plane by scanning the system parameter space (Fig. 6). The simulation results show that there are three regions. In region I, the stable signal propagation can be found as shown in Fig. 1; in region II, the system orbital is chaotic due to the existence of the defect points as shown in Figs. 2(b) and 4(b); region III is an isolated area surrounded by region II, and the wave can spread despite of the defect points. It is a novel signal propagation area as shown in Fig. 3.

The above three regions can be well classified by the speed of the signal propagation (propagating distance of the wave front in each time unit) and the propagation distance (the maximum distance that the propagating signal can reach). In Fig. 7, the speed and the distance each is plotted as a function of c_2. In region I, the comparatively large speed and the large propagating distance can be found. The signal probably spreads to infinity when $c_2 \to 0$ (numerical results show that the stable propagation can be obtained even when the system size is larger than $L = 10000$). In region II, the two indexes are both close to zero, indicating the failure of the signal propugation. While in region III, nonzero speed and distance are observed. The critical points for the three types of wave transmissions are clearly shown in Fig. 7.

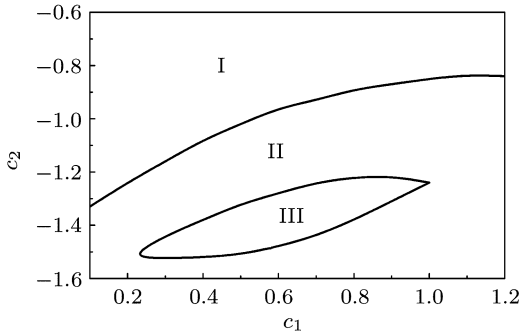


Fig. 6. Phase diagram of system in the c_1–c_2 plane. Region I denotes the parameter region for the stable signal propagating. Region II denotes the parameter area where orderly signal cannot propagate because of the defects. Region III denotes the special parameter zone where the signal propagates conquering the defects.

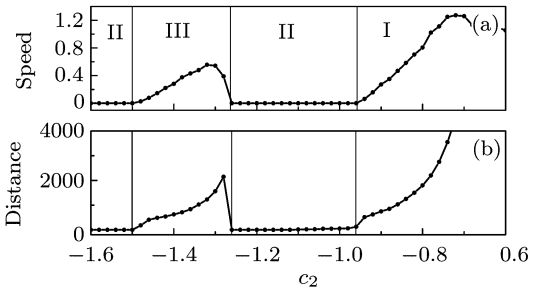


Fig. 7. (a) Wave speed and (b) maximum propagating distance versus c_2.

The stability and the generality of the above observations can be investigated by considering different initial conditions. The oscillatory frequencies with random initial conditions (the initiations for the system variable are arbitrarily chosen from −1 to 1) and the plane-wave ($A = \sqrt{1-k^2}\,\mathrm{e}^{\mathrm{i}kx}$,$k = 2\pi\, m/L$) initial conditions are compared in Fig. 8. With the control, stable frequency spectra can be found in regions I and III, while they fluctuates in region II, which confirms the observations in Fig. 7. In Fig. 8(a), the cases of the arbitrarily chosen system variable and the plane-wave initial conditions are illustrated by cross and black dot symbols, respectively. To be clearer, the differences between the frequency distributions with different initial conditions are plotted as well. In regions I and III, the corresponding frequency differences approach to zero. While in Region II, the frequency difference for two initial conditions is large, as shown in Fig. 8(b). For comparison, the frequency distribution and the difference in the absence of the wave source are plotted in Figs. 8(c) and 8(d). In this case, the failure of the signal propagation is observed in region III. In this respect, the signal propagation is dependent on the existence of the wave source, but independent of the initial configurations.

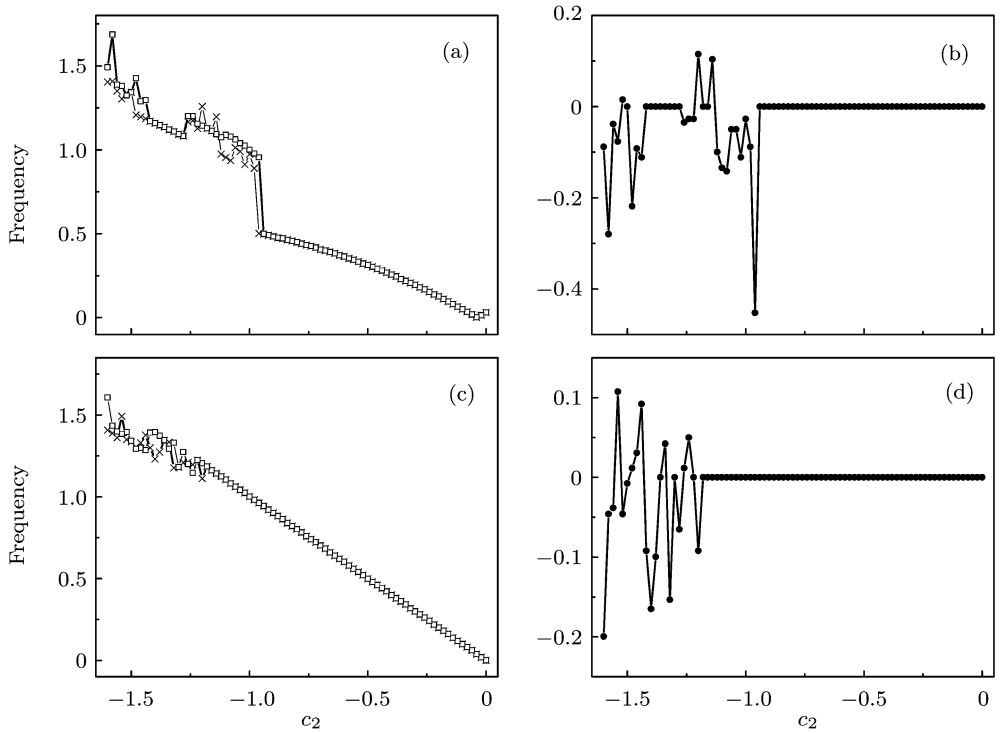


Fig. 8. Oscillatory frequencies of Re A versus c_2 under different initial conditions. The cross and the black dot denote the cases with random and plane-wave initial conditions, respectively. Panels (a) and (c) show the results with and without the control, respectively, panels (b) and (d) show the frequency differences corresponding to panels (a) and (c), respectively.

4. Conclusion

In conclusion, the signal propagation in the CGLE is studied by setting a wave source at the system boundary. Three types of signal propagations are revealed in different system parameter regions. In region I, where c_1 and c_2 have small absolute values, the signal can stably propagate, and the amplitude of the variable is nearly a constant. In region II, where c_1 and c_2 have large absolute values, the system presents defect points, and the signal propagation is prevented. In region III, which is an island-shape zone surrounded by region II, the signal can spread with a novel amplitude mode. A newly born frequency Ω_2 induced by the wave source is crucial for the signal propagation. The relevant factors, such as the propagation speed, the maximum propagating distance, and the oscillatory frequency, are studied in detail. The stability and the generality of the existence of region III are investigated by imposing different initial conditions. The finding of the amplitude wave extends the system parameter region of the wave propagation and presents a new signal transmission mode, and therefore is expected to be of much importance in the future application research.

References

[1] Kuramoto Y 1984 *Chemical Oscillations, Waves, and Turbulence* (New York: Springer)

[2] Cross M C and Hohenberg P C 1993 *Rev. Mod. Phys.* **65** 851

[3] Chate H 1994 *Nonlinearity* **7** 185

[4] Aranson I S and Kramer L 2002 *Rev. Mod. Phys.* **74** 99

[5] Goryachev A and Kapral R 1996 *Phys. Rev.* E **54** 5469

[6] Brunnet L G and Chate H 1998 *Physica* A **257** 347

[7] Zhan M and Kapral R 2006 *Phys. Rev.* E **73** 026224

[8] Bar M and Eiswirth M 1993 *Phys. Rev.* E **48** R1635

[9] Barkley D, Kness M and Tuckerman L S 1990 *Phys. Rev.* A **42** 2489

[10] Mikhailov A S and Showalter K 2006 *Phys. Rep.* **425** 79

[11] Yang R, Xie Y J, Wang Y Y and Fu H Z 2008 *Acta Phys. Sin.* **57** 5513 (in Chinese)

[12] Ding W S, Xi L and Liu L H 2008 *Acta Phys. Sin.* **57** 7705 (in Chinese)

[13] Lü Y P, Gu G F, Lu H C, Dai Y and Tang G N 2009 *Acta Phys. Sin.* **58** 7573 (in Chinese)

[14] Lü Y P, Gu G F, Lu H C, Dai Y and Tang G N 2009 *Acta Phys. Sin.* **58** 2996 (in Chinese)

[15] Li W, Liu S B and Yang W 2010 *Chin. Phys.* B **19** 030307

[16] Zamir B and Ali R 2011 *Chin. Phys.* B **20** 014102

[17] Brusch L, Zimmermann M G, van Hecke M, Bar M and Torcini A 2000 *Phys. Rev. Lett.* **85** 86

[18] Brusch L, Torcini A, van Hecke M, Zimmermann M G and Bar M 2001 *Physica* D **160** 127

[19] Brusch L, Torcini A and Bar M 2003 *Physica* D **174** 152

[20] Lan Y, Garnier N and Cvitanovic P 2004 *Physica* D **188** 193

[21] Choudhury S R 2005 *Math. Comput. Simulat.* **69** 243

[22] Ipsen M, Kramer L and Srensen P G 2000 *Phys. Rep.* **337** 193

[23] Boccaletti S, Grebogi C, Lai Y C, Mancini H and Maza D 2000 *Phys. Rep.* **329** 103

[24] Gao J H and Zheng Z G 2007 *Chin. Phys. Lett.* **24** 359

[25] Gao J H and Peng J H 2007 *Chin. Phys. Lett.* **24** 1614

[26] Gao J H, Xie L L, Zou W and Zhan M 2009 *Phys. Rev.* E **79** 056214

[27] Gao J H, Xie L L and Peng J H 2009 *Acta Phys. Sin.* **58** 5218 (in Chinese)

[28] Xie L L and Gao J H 2010 *Chin. Phys.* B **19** 060516

[29] Zhan M, Zou W and Liu X 2010 *Phys. Rev.* E **81** 036211

[30] Shraiman B I, Pumir A, van Saarloos W, Hohenberg P C, Chate H and Holen M 1992 *Physica* D **57** 241

[31] Aranson I, Levine H and Tsimring L 1994 *Phys. Rev. Lett.* **72** 2561

[32] Ipsen M and van Hecke M 2001 *Physica* D **160** 103

[33] Gao J H, Xie L L, Nie H C and Zhan M 2010 *Chaos* **20** 043132